

The Power of Low Noise in IoT Smart Sensors

Mark Looney
Analog Devices, Inc.

Introduction

Performance vs. power dissipation; it's one of the most delicate trade-offs for those who are developing smart sensors for the emerging IoT-based application space. Within the broad space of performance, noise is often an important attribute to evaluate, as it can constrain component selection for key functional blocks in a smart sensor, which in turn can increase the power burden. In addition, noise behaviors can drive filtering requirements, which can influence the sensor's responsiveness to rapid changes in conditions and extend the time it takes to develop a quality measurement.

In applications that support continuous observation (sampling, processing, communication), system architects often have to work through an adversarial relationship between noise and power, as the lowest noise solutions are rarely the ones that also offer the lowest power (within a particular functional class of devices). For example, MEMS accelerometers commonly serve as a core sensor in remote tilt measurement systems. Table 1 captures the highlights from two different products that offer industry-leading performance in either noise or power at this time: [ADXL355](#) (low noise) and [ADXL362](#) (low power).

Table 1. MEMS Accelerometer Comparison

Device/Mode	Noise Density ($\mu g/\sqrt{Hz}$)	Voltage (V)	Current (μA)	Power (μW)
ADXL355	20	2.25	150	337.5
ADXL362/Ultralow Noise	175	2.0	13	26
ADXL362/Low Noise	400	2.0	3.3	6.6
ADXL362/Low Power	550	2.0	1.8	3.6

Three of the four entries in Table 1 represent selectable modes of operation in the ADXL362, while the fourth entry represents the key metrics for the ADXL355. Starting with the key boundaries of this trade space, the ADXL355 offers nearly 27 times lower noise than the lowest power mode in the ADXL362, but at much higher power dissipation. For an application that has more challenging performance requirements, which may require consideration of the highest performance mode in the ADXL362, the ADXL355's noise will be nine times lower, while the ADXL362's power dissipation will be 13 times lower.

When supporting an application that will not require continuous observation and measurements, the relationship between average power dissipation and noise gets more interesting. The relationship between noise and power dissipation can even become complementary, which may seem surprising for some. For some, this is great news as previous generation designs may have been delayed while developers struggled to determine if power or performance should drive their design. Now, rather than waiting for someone else to answer that same old question, smart sensor architects are pressing to redefine their own work by quantifying relevant options within this trade space, on their own.

Smart Sensor Architecture

Quantifying relevant options for a particular application starts with making some assumptions about the signal chain, so that this can start with a conceptual architecture. Figure 1 provides a generic example of a smart sensor's architecture that contains the most common functions.

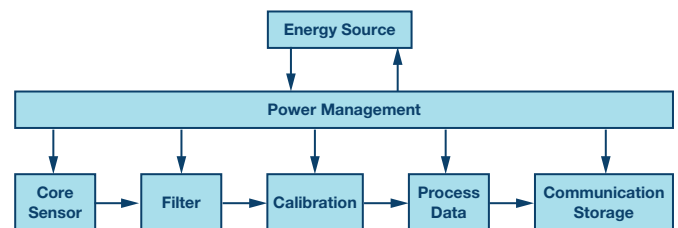


Figure 1. Smart sensor architecture.

Sensor Core

The signal chain in a smart sensor node starts with the core sensor function. In its most basic form, the core sensor is also known as a transducer, which translates a physical condition or property into a representative electrical signal. A transducer's scale factor describes the linear portion of its electrical response to the physical property or condition that it is monitoring. For example, a temperature sensor with an analog output, such as the [AD590](#), will offer a scale factor in units of mV/°C. A digital accelerometer, such as the [ADXL355](#), will offer its scale factor in terms of LSBs/g or codes/g.

Filter

The next functional block in the signal chain (Figure 1) is the filter. The purpose of this stage is to reduce noise from frequency bands that the core sensor may support, but are not relevant in the application. In a vibration monitoring application, this may be a band-pass filter that separates random vibration from a specific spectral signature that can indicate degradation of a machine’s health. In a tilt sensor, this can be a simple low-pass filter, such as a running average. In this case, the length of time presents an important trade-off between the settling time and the residual noise in the filter’s output. Figure 2 offers an example of an Allan variance curve for the ADXL355, which presents the uncertainty (noise) of a measurement, with respect to the averaging time that produces that measurement.

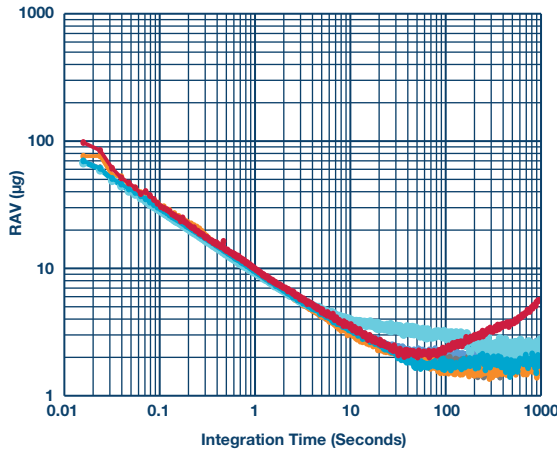


Figure 2. Allan variance curve: ADXL355 and ADXL362.

Calibration

The purpose of the calibration function is to improve the precision of the measurement through application of correction formulas. In the most demanding applications, these correction formulas typically come from direct observation of sensor responses, while they are measuring tightly controlled conditions. For example, in a tilt sensor application, the calibration process will involve observation of the MEMS accelerometer’s output in several different orientations, with respect to gravity. The general objective of these observations will be to observe the sensor response to enough orientations to resolve all 12 correction factors ($m_{11}, m_{12}, m_{13}, m_{21}, m_{22}, m_{23}, m_{31}, m_{32}, m_{33}, b_x, b_y, b_z$) in the following relationship (see Equation 1):

$$\begin{bmatrix} a_{xc} \\ a_{yc} \\ a_{zc} \end{bmatrix} = \begin{bmatrix} m_{11} & m_{12} & m_{13} \\ m_{21} & m_{22} & m_{23} \\ m_{31} & m_{32} & m_{33} \end{bmatrix} \times \begin{bmatrix} a_x \\ a_y \\ a_z \end{bmatrix} + \begin{bmatrix} b_x \\ b_y \\ b_z \end{bmatrix} \tag{1}$$

The correction factors in Equation 1 address bias, sensitivity, and alignment errors. This formula can also expand to account for higher order sensor behaviors (nonlinearity) or environmental dependencies (temperature, supply level) as well.

Data Processing

The data processing function translates calibrated and filtered sensor data into a measurement result that best supports the application. In a vibration monitoring system, this could be a simple rms-to-dc conversion or a fast Fourier transform (FFT) with spectral alarms (see ADIS16228). In a tilt sensing application, the smart sensor will translate acceleration-based responses to gravity into orientation angle estimates, using Equation 2, Equation 3, or Equation 4.

$$\theta_x = a \sin(a_x) \tag{2}$$

$$\theta_x = a \tan\left(\frac{a_x}{a_y}\right) \tag{3}$$

$$\theta_x = a \tan\left(\frac{a_x}{\sqrt{a_y^2 + a_z^2}}\right) \tag{4}$$

These three relationships represent tilt estimation with one, two, and three accelerometer measurement respectively, assuming perfect orthogonality between each of the accelerometers.

Communication/Storage

The communication/storage function supports data staging and connectivity with all IoT cloud services (encryption/security, storage, and analytics).

Power Cycling Operation

The power management (PM) function provides three different functions for a typical smart sensor. The PM’s first function is to manage all of the power sequencing requirements for all of the components in the signal chain. The PM’s second function is to convert the supply from the energy source into voltage(s) that support optimal operation in all of the components in the signal chain. Finally, in systems that have regular measurement intervals, the PM system provides scheduling to trigger each measurement event.

Power cycling is common way to identify this type of discontinuous operation in a smart sensor node. By resting in a low power (or zero power) state, in between measurement events, this technique helps conserve energy in the smart sensor. Figure 3 illustrates the instantaneous power dissipation over a complete measurement cycle for a smart sensor that is leveraging this technique.

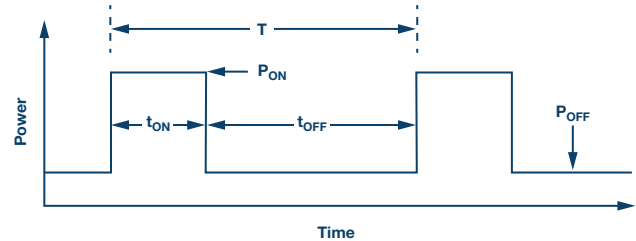


Figure 3. Basic power cycling diagram.

Equation 5 provides a simple relationship for estimating the average power dissipation (PAV), using the operational attributes from Figure 3.

$$P_{AV} = P_{ON} \frac{t_{ON}}{T} + P_{OFF} \frac{t_{OFF}}{T} \tag{5}$$

$$T = t_{ON} + t_{OFF}$$

P_{ON} is the average power dissipation in the smart sensor node when it is sampling and processing data to produce and communication a relevant measurement result.

P_{OFF} is the average power dissipation that the smart sensor node requires to support its low power sleep mode.

t_{ON} is the time that it takes the smart sensor to turn on, produce a measurement result, communicate that result to the IoT cloud, and turn back off.

t_{OFF} is the time that the smart sensor is dormant (sleep mode or completely powered off).

T is the average measurement cycle time.

Measurement Process

During its on time (t_{ON}), a smart sensor will typically work through several different operational states. Figure 4 and Equation 6 offer an example sequence, which breaks the on time down into four different segments: initialization, settling, processing, and communication.

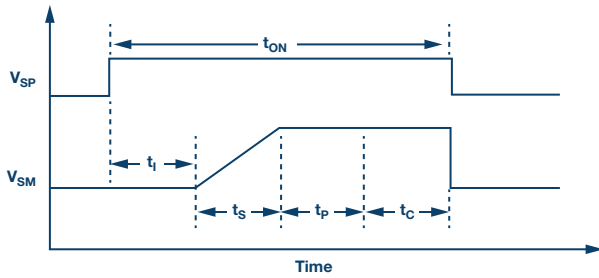


Figure 4. Smart sensor measurement cycle sequence.

$$t_{ON} = t_i + t_s + t_p + t_c + \quad (6)$$

t_i is the initialization time, which represents the time between power application (V_{SP}) and the time when each component in the signal chain is ready to support data sampling and processing.

t_s is the settling time, which represents the time between the first data sample and the time that the filter's output (V_{SM}) has settled to a sufficient level of accuracy.

t_p is the processing time, which represents the time it takes to produce the measurement result, after the filter settles. This can include application of calibration formulas, application-specific signal processing, and data encryption for the IoT security protocol.

t_c is the communication time, which represents the time it takes to connect with the cloud services, transmit the encrypted data, and support any error checking or authentication services.

Settling Time Influence

Using the segmentation of the different phases in a measurement cycle (Figure 4), the settling time of the filter is an obvious area where noise can influence the power dissipation in a power cycling, smart sensor node. In general, the decrease in noise magnitude that comes from averaging is proportional to the square root of the averaging time, while the increase in energy consumption is directly proportional to the averaging time. So reducing the noise magnitude by a factor of 10 will cause the energy consumption (during filter settling) to increase by a factor of 100! This type of disproportional trade-off can quickly favor the sensor that requires the least amount of filtering (lowest noise).

Application Example

Consider the microwave antenna platform in Figure 5, which rests on a tower platform. In this type of communication system, the reliability of the data link depends on the accuracy of the pointing angle. Maintaining the pointing angle can require manual adjustment, especially after earthquakes and other disturbances to the platforms that these antennas rest on. Since this type of remote maintenance can be costly and limited in response time, one antenna operator is investigating the feasibility of using MEMS accelerometer to monitor changes in orientation of the antenna body as part of their maintenance response strategy.

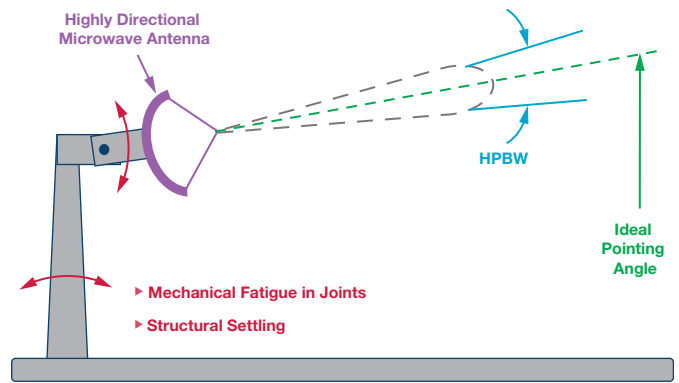


Figure 5. Microwave antenna platform.

The system architect starts this investigation with their most basic functional requirement: maintain reliable communications on each antenna platform. In this system, reliable data communications requires that the antenna's pointing angle must stay within the antenna's half power beamwidth (HPBW, see Figure 5) at all times. Therefore, they determine that they would like to trigger a maintenance visit when the antenna's orientation change by 25% of the antenna's HPBW, over a short period of time.

Within the error budget for supporting this goal, the architect allows for the peak noise in the tilt measurement to be 10% of the measurement objective (25% of HPBW). For simplicity, the architect also assigns the peak value of the noise to be equal to three times greater than the root mean square (rms) value of the noise. Equation 7 captures all of these defining inputs and simplifies it into one relationship, which simply states that noise in the tilt measurement needs to be 120 times lower than the HPBW.

$$\begin{aligned} \theta_{NOISE} &< \frac{0.25 \times HPBW}{10 \times 3} \\ \theta_{NOISE} &< \frac{HPBW}{120} \end{aligned} \quad (7)$$

In order to relate this angle noise requirement to the same performance metric in the MEMS accelerometer, Equation 8 comes from plugging the result of Equation 7 into the basic accelerometer to tilt formula in Equation 2.

$$\begin{aligned} a_{NOISE} &< a \sin(\theta_{NOISE}) \\ a_{NOISE} &< a \sin\left(\frac{HPBW}{120}\right) \end{aligned} \quad (8)$$

So, for an antenna that has a HPBW of 0.7° , the noise in the accelerometer must be less than $100 \mu g$, in order to meet the existing criteria.

$$\begin{aligned} a_{NOISE} &< a \sin\left(\frac{HPBW}{120}\right) \\ a_{NOISE} &< a \sin\left(\frac{0.7}{120}\right) \\ a_{NOISE} &< 0.0001g \end{aligned} \quad (9)$$

This result establishes a metric to use in determining the amount of averaging time that each candidate sensor (from Table 1) would need, in order to achieve $100 \mu g$ of uncertainty in a measurement. Reviewing Figure 2 reveals that the ADXL355 will require an averaging time of ~ 0.01 seconds ($t_{s355} = 0.01$, see Equation 10) to get below this level.

For a quick approximation, one can assume that since the ADXL362's noise is nine times greater than the ADXL355, it will require an averaging time that is 81 times that of the ADXL355 ($t_{S362} = 81 \times t_{S355}$, see Equation 11), in order to reach the same objective. Equation 10 captures the energy consumption that comes from the settling time in the ADXL355 and Equation 11 captures the energy consumption that comes from the settling time of the ADXL362 (see Table 1).

$$E_{ADXL355} = t_{S355} \times V_{MIN355} \times I_{355} \quad (10)$$

$$E_{ADXL355} = 0.01 \text{ s} \times 2.25 \text{ V} \times 0.00015 \text{ A} = 3.38 \text{ } \mu\text{J}$$

$$E_{ADXL362} = t_{S362} \times V_{MIN362} \times I_{362} \quad (11)$$

$$E_{ADXL355} = 81 \times t_{S362} \times V_{MIN362} \times I_{362}$$

$$E_{ADXL362} = 81 \times 0.01 \text{ s} \times 2 \text{ V} \times 0.000013 \text{ A} = 21.1 \text{ } \mu\text{J}$$

Ironically, the lowest energy consumption for this level of noise performance comes from using the lowest noise accelerometer, not the lowest power accelerometer. Equation 12 divides the energy estimates for each sensor in Equation 10 and Equation 11, by the measurement interval ($T = 10$ seconds), in order to estimate the settling time's contribution to power dissipation.

$$P_{ADXL355} = \frac{E_{ADXL355}}{T} = \frac{3.38 \text{ } \mu\text{J}}{10 \text{ sec}} = 0.338 \text{ } \mu\text{W} \quad (12)$$

$$P_{ADXL362} = \frac{E_{ADXL362}}{T} = \frac{21.1 \text{ } \mu\text{J}}{10 \text{ sec}} = 2.11 \text{ } \mu\text{W}$$

Conclusion

This particular discussion has revealed a specific scenario, where the lowest power solution came from using the core sensor with the lowest noise, not the one that provides the lowest power dissipation. For those who are developing smart sensor concepts for an emerging class of IoT applications, which have demanding performance requirements and limited access to energy sources, this type of solution path could present an important lesson. In essence, clever solutions may be available for those who are willing to first understand, then challenge even the most fundamental paradigms. Sometimes, the best performance and the lowest power dissipation could actually come from the same sensor.

About the Author

Mark Looney [mark.looney@analog.com] is an *i*Sensor® applications engineer at Analog Devices in Greensboro, North Carolina. Since joining ADI in 1998, he has accumulated experience in sensor-signal processing, high speed analog-to-digital converters, and dc-to-dc power conversion. He earned B.S. (1994) and M.S. (1995) degrees in electrical engineering from the University of Nevada, Reno, and has published several articles. Prior to joining ADI, he helped start IMATS, a vehicle electronics and traffic solutions company, and worked as a design engineer for Interpoint Corporation.

Online Support Community



Engage with the Analog Devices technology experts in our online support community. Ask your tough design questions, browse FAQs, or join a conversation.

Visit ez.analog.com

Analog Devices, Inc. Worldwide Headquarters

Analog Devices, Inc.
One Technology Way
P.O. Box 9106
Norwood, MA 02062-9106
U.S.A.
Tel: 781.329.4700
(800.262.5643, U.S.A. only)
Fax: 781.461.3113

Analog Devices, Inc. Europe Headquarters

Analog Devices GmbH
Otto-Aicher-Str. 60-64
80807 München
Germany
Tel: 49.89.76903.0
Fax: 49.89.76903.157

Analog Devices, Inc. Japan Headquarters

Analog Devices, KK
New Pier Takeshiba
South Tower Building
1-16-1 Kaigan, Minato-ku,
Tokyo, 105-6891
Japan
Tel: 813.5402.8200
Fax: 813.5402.1064

Analog Devices, Inc. Asia Pacific Headquarters

Analog Devices
5F, Sandhill Plaza
2290 Zuchongzhi Road
Zhangjiang Hi-Tech Park
Pudong New District
Shanghai, China 201203
Tel: 86.21.2320.8000
Fax: 86.21.2320.8222

©2016 Analog Devices, Inc. All rights reserved. Trademarks and registered trademarks are the property of their respective owners. Ahead of What's Possible is a trademark of Analog Devices. TA15037-0-9/16

analog.com



AHEAD OF WHAT'S POSSIBLE™